

## Crystalline electric field effects in the filled skutterudite compound $\text{PrOs}_4\text{P}_{12}$

This article has been downloaded from IOPscience. Please scroll down to see the full text article.

2007 J. Phys.: Condens. Matter 19 076212

(<http://iopscience.iop.org/0953-8984/19/7/076212>)

View [the table of contents for this issue](#), or go to the [journal homepage](#) for more

Download details:

IP Address: 129.252.86.83

The article was downloaded on 28/05/2010 at 16:07

Please note that [terms and conditions apply](#).

# Crystalline electric field effects in the filled skutterudite compound $\text{PrOs}_4\text{P}_{12}$

W M Yuhasz<sup>1,2</sup>, P-C Ho<sup>2</sup>, T A Sayles<sup>2,3</sup>, T Yanagisawa<sup>2</sup>, N A Frederick<sup>2,3</sup>,  
M B Maple<sup>1,2,3</sup>, P Rogl<sup>4</sup> and G Giester<sup>5</sup>

<sup>1</sup> Materials Science and Engineering Program, University of California, San Diego, La Jolla, CA 92093, USA

<sup>2</sup> Institute for Pure and Applied Physical Sciences, University of California, San Diego, La Jolla, CA 92093, USA

<sup>3</sup> Department of Physics, University of California, San Diego, La Jolla, CA 92093, USA

<sup>4</sup> Institut für Physikalische Chemie, Universität Wien, A-1090 Wien, Währingerstr. 42, Austria

<sup>5</sup> Institut für Mineralogie und Kristallographie, Universität Wien, A-1090 Wien, Althanstr. 14, Austria

Received 20 November 2006, in final form 5 January 2007

Published 2 February 2007

Online at [stacks.iop.org/JPhysCM/19/076212](http://stacks.iop.org/JPhysCM/19/076212)

## Abstract

The filled skutterudite compound  $\text{PrOs}_4\text{P}_{12}$  was synthesized in single-crystal form using a molten metal flux growth technique. Low-temperature magnetization, specific heat, and electrical resistivity measurements showed no indication of a phase transition down to 0.1 K but had features indicative of crystalline electric field (CEF) effects. Analyses of these features in terms of a cubic CEF suggest a  $\Gamma_1$  singlet or a  $\Gamma_3$  doublet ground state separated by 30–50 K from a  $\Gamma_5$  triplet first excited state.

## 1. Introduction

The filled skutterudites have the chemical formula  $\text{MT}_4\text{X}_{12}$  ( $M$  = alkali metal, alkaline-earth, lanthanide, or actinide;  $T$  = Fe, Ru, or Os; and  $X$  = P, As, or Sb). Current interest in the filled skutterudites is motivated by the wide range of strongly correlated electron behaviour that these compounds exhibit at low temperatures. Among the filled skutterudites, the Pr-based systems, in particular, have attracted a considerable amount of attention in recent years, as a result of the discoveries of heavy fermion superconductivity in  $\text{PrOs}_4\text{Sb}_{12}$  [1, 2], antiferroquadrupolar ordering in  $\text{PrFe}_4\text{P}_{12}$  [3, 4], and a metal–insulator transition in  $\text{PrRu}_4\text{P}_{12}$  [5].

Various measurements performed on the filled skutterudites reveal features that have been interpreted in terms of crystalline electric field (CEF) effects [1, 3, 6–9]. These features range from Schottky anomalies in the specific heat [1] to deviations of the inverse magnetic susceptibility from Curie–Weiss behaviour at temperatures comparable to the CEF splittings between the  $\text{Pr}^{3+}$  energy levels [6]. In developing an understanding of the various types of phenomena exhibited by the Pr-based filled skutterudite compounds, it is important to determine the  $\text{Pr}^{3+}$  energy level scheme and how it depends on structure and composition.

For instance, measurements of the physical properties of the filled skutterudite compound  $\text{PrOs}_4\text{Sb}_{12}$ , which represents the first Pr-based heavy fermion superconductor, display features that reflect strong CEF effects [1, 8, 9]. A complete picture of the CEF splitting in  $\text{PrOs}_4\text{Sb}_{12}$  may shed light on how the heavy fermion behaviour and unconventional superconductivity occur in this system. This approach can be extended to include a comparison of the physical properties of various Pr-based filled skutterudites and their associated CEF effects, which may lead to a more general understanding of how strongly correlated electron behaviour develops in these compounds. With this in mind, the filled skutterudite compound  $\text{PrOs}_4\text{P}_{12}$  was considered for study. Previous measurements of polycrystalline  $\text{PrOs}_4\text{P}_{12}$  showed no indication of a phase transition down to 1.7 K [5, 10]. In this paper, we present new measurements on single crystals of  $\text{PrOs}_4\text{P}_{12}$  to determine the CEF energy level scheme and to check for magnetic or quadrupolar ordering below 1.7 K.

## 2. Experimental details

Single crystals of  $\text{PrOs}_4\text{P}_{12}$  were synthesized using a molten tin flux growth technique from a mixture of elemental Pr (3N), Os (3N8), P (5N), and Sn (5N) in a ratio of 1:4:20:50. The elements were sealed in a carbon-coated quartz tube under 150 Torr ultra-high purity Ar. The sealed quartz tube was then placed in a box furnace and heated to 1130 °C for 5 days; this was followed by a slow cooling at 2 °C h<sup>-1</sup> to 600 °C. The resulting crystals typically had overall dimensions of less than 1 mm.

X-ray powder diffraction measurements were performed using a Rigaku D/MAX B x-ray machine on a powder of ground single crystals. Further x-ray structural refinement was performed on two single crystals with similar dimensions. The x-ray intensity data were collected on a four-circle Nonius Kappa diffractometer equipped with a CCD area detector employing graphite-monochromated Mo K $\alpha$  radiation ( $\lambda = 0.071\,073$  nm). Orientation matrix and unit cell parameters were derived using the program DENZO [11]. No absorption corrections were necessary because of the rather regular shape and small dimensions of the investigated crystals. The structure was refined with the aid of the SHELXS-97 program [12].

Magnetization measurements were performed using a Quantum Design Magnetic Properties Measurement System (MPMS) in magnetic fields,  $H$ , up to 5.5 T for 1.7 K  $\leq T \leq 300$  K. Electrical resistivity  $\rho(H, T)$  measurements were made using a four-probe ac technique for 2 K  $\leq T \leq 300$  K in fields up to 8 T in a Quantum Design Physical Properties Measurement System (PPMS) with a constant current of 1 mA and for 0.1 K  $\leq T \leq 2.6$  K in fields up to 8 T using a <sup>3</sup>He–<sup>4</sup>He dilution refrigerator with a constant current of 300  $\mu$ A. Specific heat  $C(T)$  measurements on  $\text{PrOs}_4\text{P}_{12}$  were performed for 0.5 K  $\leq T \leq 90$  K in a semi-adiabatic <sup>3</sup>He calorimeter on a collection of single crystals with a total mass of 80 mg.

## 3. Results

The x-ray powder diffraction pattern indicates that  $\text{PrOs}_4\text{P}_{12}$  is single phase with no major impurity peaks and a cubic unit cell parameter  $a = 8.0751(5)$  Å, in good agreement with a previous measurement, where  $a = 8.0710(10)$  Å [13]. The single-crystal structural refinement confirmed that  $\text{PrOs}_4\text{P}_{12}$  possesses a  $\text{LaFe}_4\text{P}_{12}$ -type structure (space group  $Im\bar{3}$ ) with two formula units per unit cell, and  $a = 8.080(1)$  Å. The crystal structure parameters, from the structural refinement of  $\text{PrOs}_4\text{P}_{12}$ , are listed in table 1.

The dc magnetic susceptibility  $\chi_{\text{dc}}$  and inverse dc magnetic susceptibility  $\chi_{\text{dc}}^{-1}$  versus  $T$ , measured in a magnetic field of 500 Oe, between 2 and 300 K, are displayed in figure 1. A Curie–Weiss fit to the  $\chi_{\text{dc}}^{-1}(T)$  data from 100 to 250 K yields an effective moment

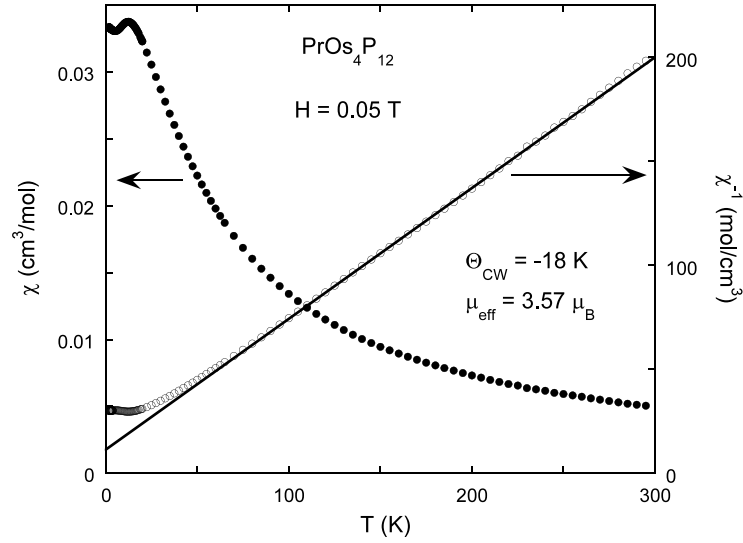


**Figure 1.** The dc magnetic susceptibility  $\chi_{dc}$  (solid circles) and  $\chi_{dc}^{-1}$  (open circles) versus temperature  $T$  at  $H = 0.05$  T for  $\text{PrOs}_4\text{P}_{12}$ . The straight line is a Curie-Weiss fit to  $\chi_{dc}^{-1}(T)$ .

**Table 1.** Single-crystal structural data for  $\text{PrOs}_4\text{P}_{12}$  (LaFe<sub>4</sub>P<sub>12</sub>-type, space group  $Im\bar{3}$ ; No. 204) taken at  $T = 296$  K, with a scattering angle range of  $2^\circ < 2\theta < 80^\circ$ .

PrOs <sub>4</sub> P <sub>12</sub>		
Crystal size $60 \times 74 \times 83 \mu\text{m}^3$	Lattice parameter (Å) $a = 8.080(1)$	Density (g cm <sup>-3</sup> ) $\rho = 8.017$
Reflections in refinement $286 \geq 4\sigma(F_0)$ of 322	Number of variables = 12 Goodness of fit = 1.068	$R_F^2 = \sum  F_0^2 - F_c^2  / \sum F_0^2$ = 0.0156
Pr in 2a (0, 0, 0); Occupancy = 1.02(2)	Thermal displacements (Å <sup>2</sup> ) Pr: $U_{11} = U_{22} = U_{33}$ = 0.0079(1)	Interatomic distances (Å) Pr-12 P 3.1091
Os in 8c (1/4, 1/4, 1/4); Occupancy = 1.00(1)	Thermal displacements (Å <sup>2</sup> ) Os: $U_{11} = U_{22} = U_{33}$ = 0.0004(1)	Interatomic distances (Å) Os-6 P 2.3617
P in 24g (0, y, z); y: 0.14304(6) z: 0.35722(6) Occupancy = 1.00(1)	Thermal displacements (Å <sup>2</sup> ) P: $U_{11} = 0.0017(2)$ $U_{22} = 0.0023(2)$ $U_{33} = 0.0028(2)$	Interatomic distances (Å) P-1 P 2.3073 -1 P 2.3115 -2 Os 2.3617 -1 Pr 3.1091

$\mu_{\text{eff}} = 3.57\mu_{\text{B}}/\text{f.u.}$  and a Curie-Weiss temperature  $\Theta_{\text{CW}} = -18$  K. This value of  $\mu_{\text{eff}}$  is close to the  $\text{Pr}^{3+}$  free-ion value of  $3.58\mu_{\text{B}}/\text{f.u.}$  as well as the value of  $3.63\mu_{\text{B}}/\text{f.u.}$  previously found for polycrystalline  $\text{PrOs}_4\text{P}_{12}$  [5]. At low temperatures,  $\chi_{dc}^{-1}(T)$  deviates from a Curie-Weiss law, while  $\chi_{dc}(T)$  develops a broad peak centred at 12 K. This peak is much more pronounced than the feature observed in the  $\chi(T)$  data for polycrystalline  $\text{PrOs}_4\text{P}_{12}$  and is a strong indication of CEF effects [5], which will be discussed in more detail in section 4.

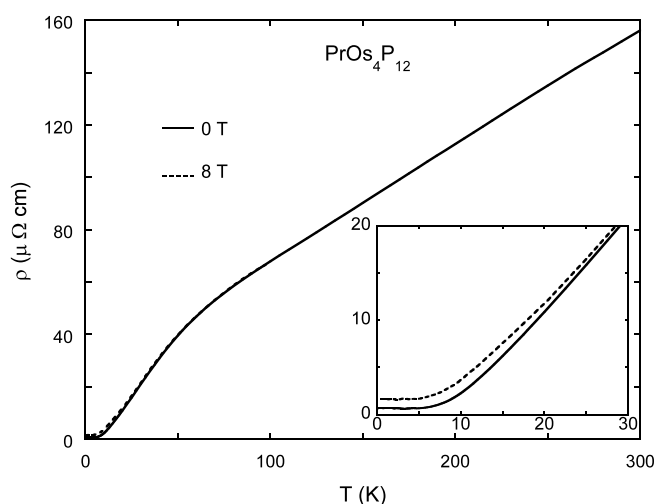


**Figure 2.** Electrical resistivity  $\rho$  versus  $T$  for  $\text{PrOs}_4\text{P}_{12}$  at  $H = 0$  and 8 T. The inset displays the low-temperature behaviour below 50 K.

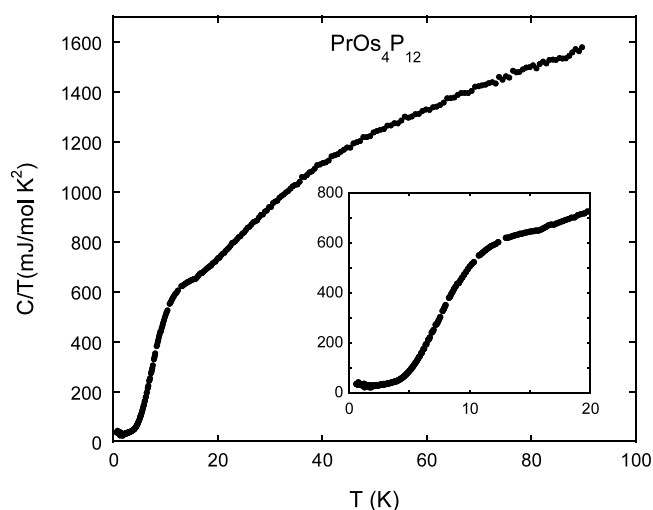


**Figure 3.** Specific heat  $C$  divided by temperature  $T$  versus  $T$  for  $\text{PrOs}_4\text{P}_{12}$ . The inset reveals the low-temperature behaviour of  $C(T)/T$  below 20 K.

Displayed in figure 2 are electrical resistivity  $\rho(T)$  data for a  $\text{PrOs}_4\text{P}_{12}$  single crystal with a residual resistivity ratio  $\sim 180$  between 0.1 and 300 K at  $H = 0$  and 8 T. In zero field,  $\rho(T)$  displays a linear decrease from 300 to 75 K, followed by a rapid downturn that approaches a constant value of  $0.65 \mu\Omega \text{ cm}$  below 5.5 K. Except for a small positive magnetoresistance below 30 K, the behaviour of  $\rho(T)$  does not change in applied fields up to 8 T. The specific heat  $C$  divided by temperature  $T$  versus  $T$  data for  $\text{PrOs}_4\text{P}_{12}$  from 0.6 to  $\sim 80$  K are shown in figure 3. The only clear feature is a Schottky-like shoulder centred around 13 K (inset to figure 3), which gives further evidence for CEF effects in  $\text{PrOs}_4\text{P}_{12}$ . The  $C(T)/T$  data below the shoulder decrease to a value of  $\sim 32 \text{ mJ mol}^{-1} \text{ K}^{-2}$ .

#### 4. Discussion

The  $T$ -dependences of  $\chi_{\text{dc}}$ ,  $\rho$ , and  $C/T$  of  $\text{PrOs}_4\text{P}_{12}$  reveal features that indicate the presence of strong CEF effects. These features can be fitted by expressions that depend on the CEF splitting scheme and provide more information about the  $\text{Pr}^{3+}$  ion ground and excited states

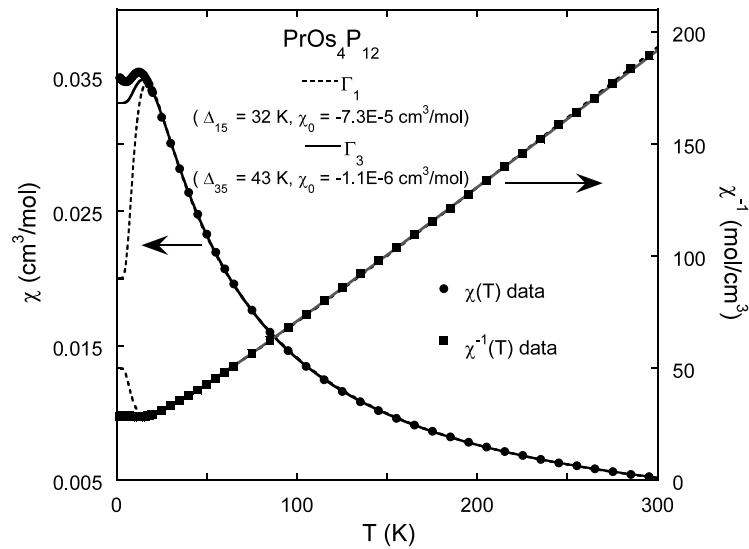


**Figure 4.** Fits of  $\chi_{dc}(T)$  (solid circles) and  $\chi_{dc}^{-1}(T)$  (solid squares) by CEF models with a  $\text{Pr}^{3+}$   $\Gamma_1$  (dashed line) and  $\Gamma_3$  (solid line) ground state. See the text for explanation of the parameters indicated in the figure.

and their splittings in  $\text{PrOs}_4\text{P}_{12}$ . For simplicity, the CEF calculations were made for cubic  $O_h$  symmetry which, in zero field, closely approximate those made for the actual tetrahedral  $T_h$  symmetry of  $\text{PrOs}_4\text{P}_{12}$ . The  $\text{Pr}^{3+}$  ninefold degenerate  $J = 4$  Hund's rule ground state multiplet splits in a cubic CEF into a  $\Gamma_1$  singlet, a  $\Gamma_3$  doublet, and  $\Gamma_4$  and  $\Gamma_5$  triplets. The CEF variables used to make the fits are those developed by Lea, Leask, and Wolf (LLW), where  $X_{LLW}$  is the ratio of the fourth- and sixth-order terms of the angular momentum operators and  $W$  is an overall energy scale [14]. The lack of magnetic order above 0.1 K, as well as 2 K magnetization  $M$  versus  $H$  measurements (not shown) that indicate a magnetization of only  $0.3\mu_B/\text{f.u.}$  by 5 T, imply a nonmagnetic ground state for the  $\text{Pr}^{3+}$  ions in  $\text{PrOs}_4\text{P}_{12}$ . Given a nonmagnetic ground state, the CEF fits will be performed for the cases of both  $\Gamma_1$  singlet and  $\Gamma_3$  doublet nonmagnetic ground states.

Figure 4 shows the CEF fits to the  $\chi_{dc}(T)$  and  $\chi_{dc}^{-1}(T)$  data from 2 to 300 K assuming  $\Gamma_1$  singlet and  $\Gamma_3$  doublet nonmagnetic ground states, respectively. A constant contribution  $\chi_0$  to the magnetic susceptibility was also included to improve the quality of the fits. One possible source for this constant term is a Landau diamagnetic contribution due to atomic core electrons, estimated to be  $-8.4 \times 10^{-4} \text{ cm}^3 \text{ mol}^{-1}$  in the case of  $\text{LaFe}_4\text{P}_{12}$  [15]. The best fit with a  $\Gamma_1$  singlet ground state was found for  $X_{LLW} = 0.46$  and  $W = 4.07$ , which results in an energy level splitting of 32 K between the  $\Gamma_1$  singlet ground state and the  $\Gamma_5$  triplet first excited state. The low-temperature behaviour of the  $\chi_{dc}(T)$  data is not accurately reproduced by the CEF fit, similarly to the case of  $\text{PrOs}_4\text{Sb}_{12}$ , which was determined to possess a nonmagnetic  $\Gamma_1$  singlet ground state [16]. For the case of a nonmagnetic  $\Gamma_3$  doublet ground state, the best fit was found for  $X_{LLW} = -0.69$  and  $W = -8$ , resulting in an energy level splitting of 43 K between the  $\Gamma_3$  ground state and the  $\Gamma_5$  first excited state. Below  $\sim 15$  K, the fit assuming a  $\Gamma_3$  ground state deviates from the  $\chi(T)$  data, but not as significantly as the fit assuming a  $\Gamma_1$  ground state. The diamagnetic contribution to the CEF fits ranged from  $-1 \times 10^{-6} \text{ cm}^3 \text{ mol}^{-1}$  for the  $\Gamma_3$  ground state fit to  $-7.3 \times 10^{-5} \text{ cm}^3 \text{ mol}^{-1}$  for the  $\Gamma_1$  ground state fit; varying these values did not significantly affect the two CEF energy level schemes.

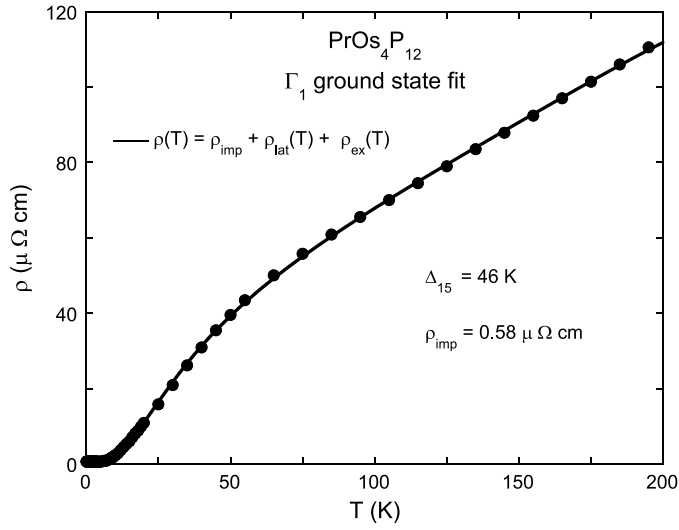


**Figure 5.** Fit to an expression based on a CEF model to the  $\rho(T)$  data using equation (1) assuming a  $\text{Pr}^{3+}$   $\Gamma_1$  ground state. See the text for explanation of the parameters indicated in the figure.

Crystalline electric field fits were also performed for the zero-field electrical resistivity data (figure 5) using the expression

$$\rho(T) = \rho_{\text{imp}}(T) + \rho_{\text{lat}}(T) + \rho_{\text{ex}}(T), \quad (1)$$

where  $\rho_{\text{imp}}$  is the residual resistivity due to scattering of electrons by impurities and defects,  $\rho_{\text{lat}}$  is the lattice contribution associated with scattering of electrons by phonons, and  $\rho_{\text{ex}}$  is the term due to s-f exchange scattering of electrons from the  $\text{Pr}^{3+}$  4f energy levels in a cubic CEF [17]. Since the addition of an aspherical Coulomb scattering term did not improve the quality of the fits to the  $\rho(T)$  data for  $\text{PrOs}_4\text{P}_{12}$ , this contribution was not included in the analysis. Identical fits to the  $\rho(T)$  data could be obtained using equation (1) and assuming either a nonmagnetic  $\Gamma_1$  singlet ground state (shown in figure 5) or a nonmagnetic  $\Gamma_3$  doublet ground state. In both fits, the contribution  $\rho_{\text{lat}}(T)$  was estimated from the  $\rho_{\text{lat}}(T)$  data of  $\text{LaOs}_4\text{P}_{12}$  below 200 K scaled by  $\sim 0.25$  [18]. The formula for the contribution  $\rho_{\text{ex}}$  was also scaled in both cases by  $\sim 2.8$ . Figure 5 features the  $\Gamma_1$  ground state fitted with  $\rho_{\text{imp}} = 0.58 \mu\Omega \text{ cm}$ , where  $\rho_{\text{ex}}$  is best described by a CEF splitting of 46 K ( $X_{\text{LLW}} = 0.38$  and  $W = 2.7$ ) between the  $\Gamma_1$  singlet ground state and the  $\Gamma_5$  triplet first excited state. A fit similar to that shown in figure 5 was also found for a  $\Gamma_3$  ground state with  $\rho_{\text{imp}} = 0.67 \mu\Omega \text{ cm}$  and  $\rho_{\text{ex}}$  best described by a CEF splitting of 55 K ( $X_{\text{LLW}} = -0.64$  and  $W = -5.2$ ) between the  $\Gamma_3$  doublet ground state and the  $\Gamma_5$  triplet first excited state.

Further evidence for a splitting of  $\sim 30$ – $50$  K between the  $\text{Pr}^{3+}$   $\Gamma_1$  or  $\Gamma_3$  nonmagnetic ground state and  $\Gamma_5$  triplet first excited state for  $\text{PrOs}_4\text{P}_{12}$  was found through fits to a Schottky-like anomaly in the  $C(T)/T$  data. In figure 6, the Schottky-like anomaly centred around 13 K was fitted from 2 to 15 K by the equation

$$C(T)/T = C_e(T)/T + C_{\text{lat}}(T)/T + AC_{\text{Sch}}(T)/T, \quad (2)$$

which includes an electronic, lattice, and two-level Schottky contributions with the following forms:  $C_e(T) = \gamma T$ ,  $C_{\text{lat}}(T) = \beta T^3$ , and  $C_{\text{Sch}}(T) = R(\delta/T)^2(g_a/g_b)[1 + (g_a/g_b)\exp(-\delta/T)]^{-2}\exp(-\delta/T)$ , where  $g_a$  ( $g_b$ ) is the degeneracy of the ground state (first excited state),  $\delta$  is the energy level splitting, and  $A$  is a scaling factor. The best fit shown in

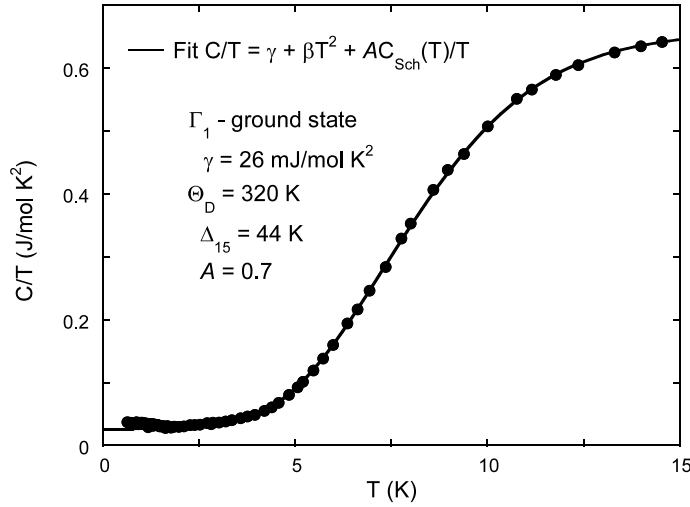


**Figure 6.** A fit using equation (2) to the  $C(T)/T$  data assuming a  $\text{Pr}^{3+}$   $\Gamma_1$  ground state. See the text for explanation of the parameters indicated in the figure.

figure 6 for a  $\Gamma_1$  singlet ground state and a  $\Gamma_5$  triplet first excited state results in an electronic specific heat coefficient  $\gamma \approx 26 \text{ mJ mol}^{-1} \text{ K}^{-2}$ , a Debye temperature  $\Theta_D \sim 320 \text{ K}$ , and a Schottky contribution scaled by  $A = 0.7$ , with an energy splitting of 44 K between the ground state and first excited state. The scaling of the Schottky anomaly required to achieve an accurate fit for a  $\Gamma_1$  singlet ground state ( $A = 0.7$ ) could be a result of significant hybridization of the localized 4f and itinerant electron states. This transfer of entropy from the localized f electrons to the conduction electrons has been observed previously in the heavy fermion superconductor  $\text{PrOs}_4\text{Sb}_{12}$  [1]. A fit identical to that shown in figure 6 was also obtained in the case of a  $\Gamma_3$  doublet ground state and a  $\Gamma_5$  triplet first excited state; the resulting best fit has an electronic specific heat coefficient  $\gamma \approx 27 \text{ mJ mol}^{-1} \text{ K}^{-2}$ , a Debye temperature  $\Theta_D \sim 354 \text{ K}$ , and a Schottky contribution scaled by  $A = 1.4$ , with an energy splitting of 43 K between the ground state and first excited state. There is no clear explanation for the large scaling parameter  $A = 1.4$  required for the best  $\Gamma_3$  ground state fit to the  $C(T)$  data, and this may be an indication that the  $\Gamma_1$  CEF scheme is more appropriate. The values of the electronic specific heat coefficient are close to that found for  $\text{LaOs}_4\text{P}_{12}$  ( $21.6 \text{ mJ mol}^{-1} \text{ K}^{-2}$ ) and less than the value of  $56.5 \text{ mJ mol}^{-1} \text{ K}^{-2}$  found for polycrystalline  $\text{PrOs}_4\text{P}_{12}$  [10]. The Debye temperature is larger than the value determined from a previous measurement of the specific heat of polycrystalline  $\text{PrOs}_4\text{P}_{12}$  which yielded  $\Theta_D = 285 \text{ K}$  [10]. One possible source for the discrepancy between the values of  $\gamma$  for polycrystalline and single-crystal  $\text{PrOs}_4\text{P}_{12}$  is tin inclusions in the single crystals, which would result in an overestimate of the  $\text{PrOs}_4\text{P}_{12}$  mass, although no indication of a tin superconducting transition at 3.72 K was observed in  $C(T)$  measurements.

After performing the various CEF fits to the magnetic susceptibility, electrical resistivity, and specific heat data, we have concluded that there are two possible CEF schemes for  $\text{PrOs}_4\text{P}_{12}$ . Our CEF splitting schemes assuming a  $\Gamma_1$  ground state are in agreement with CEF fits by Matsuhira *et al* using tetrahedral symmetry  $T_h$ , which yielded a splitting of  $\sim 48 \text{ K}$  between a nonmagnetic  $\Gamma_1$  singlet ground state and the triplet first excited state for polycrystalline  $\text{PrOs}_4\text{P}_{12}$  [10]. A potential nonmagnetic  $\Gamma_3$  doublet ground state was discounted by Matsuhira *et al*, who performed  $C(T)$  measurements in an applied magnetic field and looked



for an additional Schottky contribution to  $C(T)$  due to Zeeman splitting of the  $\Gamma_3$  doublet ground state [10]. These  $C(T)$  measurements, in fields up to 5 T, revealed no significant change in  $C(T)$  down to 1.8 K [10]. In order to confirm the proposed CEF splitting scenario, further experiments, such as inelastic neutron scattering in high fields, are required.

## 5. Summary

Measurements on  $\text{PrOs}_4\text{P}_{12}$  single crystals do not show any indication of a phase transition even at temperatures as low as 0.1 K. This is in marked contrast to the wide variety of phase transitions that occur at low temperatures in other Pr-based filled skutterudites that include conventional BCS superconductivity, unconventional superconductivity, heavy fermion behaviour, non-Fermi liquid behaviour, magnetic order, quadrupolar order, and metal–insulator transitions. Features found in the temperature dependences of the magnetic susceptibility, electrical resistivity, and specific heat can be interpreted in terms of crystalline electric field effects. CEF fits to these various features indicate a  $\Gamma_1$  or  $\Gamma_3$  nonmagnetic ground state separated by 30–50 K from a  $\Gamma_5$  first excited state, although previous work suggests that the  $\Gamma_3$  ground state CEF splitting scheme is a less likely scenario.

## Acknowledgments

We would like to thank Stella K Kim for her help with the sample preparation. The preparation of the  $\text{PrOs}_4\text{P}_{12}$  single-crystal specimens was funded by the US Department of Energy under Grant No. DE-FG02-04ER46105. The electrical resistivity, magnetization, and calorimetry investigation was supported by the US National Science Foundation under Grant No. DMR 0335173. One of the authors (TY) was supported by a JSPS Postdoctoral Fellowship for Research Abroad.

## References

- [1] Bauer E D, Frederick N A, Ho P-C, Zapf V S and Maple M B 2002 *Phys. Rev. B* **65** 100506(R)
- [2] Maple M B, Ho P-C, Zapf V S, Frederick N A, Bauer E D, Yuhasz W M, Woodward F M and Lynn J W 2002 *J. Phys. Soc. Japan* **71** (Suppl.) 23
- [3] Aoki Y, Namiki T, Matsuda T D, Abe K, Sugawara H and Sato H 2002 *Phys. Rev. B* **65** 064446
- [4] Hao L, Iwasa K, Nakajima M, Kawana D, Kuwahara K, Kohgi M, Sugawara H, Matsuda T D, Aoki Y and Sato H 2003 *Acta Phys. Pol. B* **34** 1113
- [5] Sekine C, Uchiumi T and Shirotni I 1997 *Phys. Rev. Lett.* **79** 3218
- [6] Torikachvili M S, Chen J W, Dalichaouch Y, Guertin R P, McElfresh M W, Rossel C, Maple M B and Meisner G P 1987 *Phys. Rev. B* **36** 8660
- [7] Sekine C, Inaba T, Shirotni I, Yokoyama M, Amitsuka H and Sakakibara T 2000 *Physica B* **281** 303
- [8] Frederick N A and Maple M B 2003 *J. Phys.: Condens. Matter* **15** 4789
- [9] Frederick N A, Sayles T A and Maple M B 2005 *Phys. Rev. B* **71** 064508
- [10] Matsuhira K, Doi U, Wakeshima M, Hinatsu Y, Kihou K, Sekine C and Shirotni I 2005 *Physica B* **359–361** 977
- [11] *Nonius Kappa CCD Program Package COLLECT, DENZO, SCALEPACK, SORTAV* 1998 (Delft: Nonius)
- [12] Sheldrick G M 1997 *SHELXS-97, Program for Crystal Structure Refinement* (Germany: University of Göttingen) Windows version by McArdle (Galway: National University of Ireland)
- [13] Jeitschko W and Braun D J 1977 *Acta Crystallogr. B* **33** 3401
- [14] Lea K R, Leask M J M and Wolf W P 1962 *J. Phys. Chem. Solids* **23** 1381
- [15] Meisner G P, Stewart G R, Torikachvili M S and Maple M B 1984 *Proc. 17th Int. Conf. on Low Temperature Physics* (Amsterdam: North-Holland)
- [16] Goremychkin E A, Osborn R, Bauer E D, Maple M B, Frederick N A, Yuhasz W M, Woodward F M and Lynn J W 2004 *Phys. Rev. Lett.* **93** 157003
- [17] Andersen N H, Gregers-Hansen P E, Holm E, Smith H and Vogt O 1974 *Phys. Rev. Lett.* **32** 1321
- [18] Shirotni I, Adachi T, Tachi K, Todo S, Nozawa K, Tagi T and Kinoshita M 1996 *J. Phys. Chem. Solids* **57** 211